Ab initio study of the effect of hydrogen passivation on boron-oxygen-carbon related defect complexes in silicon.

Abdulgaffar Abdurrazaq[a,b,*], Abdulrafiu T. Raji[c,**], Walter. E. Meyer[a]

[a] *Department of Physics, University of Pretoria, Pretoria 0002, South Africa.*
[b] *Ibrahim Shehu Shema Centre For Renewable Energy Research, Umaru Musa Yar'adua University, Dutsin-ma Road P.M.B. 2218 Katsina, Nigeria*
[c] *College of Science, Engineering and Technology (CSET), University of South Africa (UNISA), Florida 1709, South Africa.*

Abstract

We present hybrid density functional theory (DFT) study of defect complexes formed by oxygen, boron and carbon, in ion-implanted and electron-irradiated Czrolaski (CZ) silicon containing boron. The effect of hydrogen passivation on the defect complexes is also studied.The defects considered are the interstitial boron-interstital oxygen (B_iO_i) complex as well as interstitial boron-substitutional carbon (B_iC_s) complex, which are found in ion-implanted Czochralski silicon. Other defect complexes which are found in electron-irradiated CZ silicon and have been studied are the interstitial boron (B_i), substitutional boron-interstitial oxygen (B_sO_i), substitutional boron-interstitial boron (B_sB_i), interstitial boron-interstitial oxygen dimer(B_iO_{2i}), and substitutional boron-interstitial oxygen dimer (B_sO_{2i}).We found the defects to be stable in neutral charge state with the stability of the B_i, B_iO_i, B_sB_i, B_iO_{2i} and B_sO_{2i} increasing after hydrogen passivation. However, the stability of B_sO_i and B_iC_s defect complexes decreases after the hydrogen passivation. For the B_sB_i defect complex in particular, a deep donor level appeared after hydrogen passivation. Furthermore, we found a shift in the charge state transition levels in to the valence band for the donor levels, and a shift in to the conduction band for the acceptor levels for all the defects after hydrogen passivation. We compare our results with available theoretical and experimental studies.

Keywords:

Defect-complex, Charge state, Silicon, Passivation, Formation energy

1. Introduction

There are plethora of studies of defects in silicon, nevertheless, there are still many unanswered questions regarding the behaviour of these defects [1]. Amongst the well known defects, oxygen, carbon and hydrogen are the common impurities observed during ion-implantation or electron-irradiation of Czochralski-grown silicon. As a result, deeper understanding of the properties of binary or ternary defect complexes formed these impurities is important for technological applications [2]. Ion-implantation is a well-known silicon fabrication techniques which enable the formation of electrically inactive boron clusters [3] and a stable self-interstitial cluster [3]. Heat treatments during the evolution of such clusters result in the occurrence of the phenomenon called the transient enhanced diffusion (TED) [3, 4, 5]. Substitutional carbon is usually introduced to suppress the diffusion of boron [6, 7, 8]. The diffusion of boron might then occur either through interstitial [9] or kick out mechanism [10], and this require the contribution of self-interstitials. At around 240K in electron-irradiated p-type silicon, a (+1/0) donor level was observed at $E_C - 0.23$ eV (E_C is the energy of the conduction band minimum), and was associated to B_iO_i defect complex [11]. However, upon annealing between 443 K, a new defect level appears at $E_V + 0.29$ eV (E_V is the energy of the valence band maximum), that is stable up to 673 K, and the $E_C - 0.23$ eV disappears. It was suggested that B_iO_i dissociates at around 443 K such that B_i is trapped by C_s which results in the formation of B_iC_s [12]. Also when the p-type CZ silicon is annealed at low temperatures, B_sO_i complex is formed but unstable. However, upon annealing at 443 K, B_sB_i defect complex is formed which is rather an electrically inactive defect but which is able to trap an interstitial hydrogen(H_i) to form $B_sB_iH_i$ defect complex. The latter has a donor level (+1/0) at $E_V + 0.59$ eV. It should be emphasized that the presence of these defects causes a reduction of 2-3% in the efficiency of silicon solar cell [13]. The concentration of the defect complex is usually proportional to the concentration of boron and also

*Corresponding author
**Corresponding author
Email addresses: abdulfulbe@gmail.com (Abdulgaffar Abdurrazaq), tunderaji@gmail.com (Abdulrafiu T. Raji)

proportional to the square of the concentration of the oxygen [14, 15, 16]. Substitutional boron and oxygen dimer complex (i.e. B_sO_{2i}) was initially assumed to be the structure of the B−O defect complex, and that the oxygen dimer tends to diffuse towards the substitutional boron [14, 17, 18]. However, Voronkov and Falster proposed a structure of the B−O complex of the form B_iO_{2i} [19], but the complex is reported to have low formation probability. Also, interstitial oxygen dimer (O_{2i}) was found not to be mobile at room temperature but can bound with a B_i atom to form the B_iO_{2i} defect complex [13].

The preponderance of hydrogen interstitial (H_i) has been observed in many silicon fabrication processes. The hydrogen diffuses very fast and binds to native point defects thereby reducing or eliminating their electrical activity. In some cases, the H_i induces electrical activity when bonded to other defect complexes [20]. Due to the ubiquitous nature of hydrogen interstitial in both the electron-irradiated and the ion-implanted Czochralski silicon, we find it pertinent to study the defect complexes that may be formed in these fabrication processes. Thus, we first consider defect complexes of B_iO_i, B_iC_s, B_sO_i, B_sB_i, B_i, B_iO_{2i} and the B_sO_{2i} and thereafter studied the defect complexes formed after the hydrogen passivation of the respective defects. We have denoted interstitial hydrogen passivated defect complexes as: $B_iO_iH_i$, $B_iC_sH_i$, $B_sO_iH_i$, $B_sB_iH_i$, B_iH_i, $B_iO_{2i}H_i$, and the $B_sO_{2i}H_i$ defect complexes. Previous DFT studies of B_iO_i, B_iC_s, $B_sB_iH_i$, B_iO_{2i} and the B_sO_{2i} defect complexes employ the generalised gradient approximation exchange-correlation functional (GGA) [21]. Here we have used the Heyd-Scuseria-Ernzerhof (HSE) functional [22, 23] to study the defects, since both the GGA and the LDA have been shown to underestimate the band gap of semiconductors while the HSE functional is known to give a more accurate value of band gap [24, 25].

2. Computational Details

The density functional theory (DFT) calculations have been performed using the QUANTUM-ESPRESSO code [26]. The Heyd-Scuseria-Ernzerhof (HSE) functional [22, 23], with the norm-conserving pseudopotential [27, 28] were used to calculate the formation energy of the defects. Also, we have used the 216-atom silicon supercell, 45 Ry energy cut-off, and a

$2\times2\times2$ Monkhorst-Pack [29] k-point mesh for the calculations. The pseudo-potentials used were taken from a pseudopotential library, i.e., pseuo-dojjo($http://www.pseudo\text{-}dojo.org$). The approach used in calculating the energy of formation of a defect ($E^f(d,q)$) follows refs. [30, 31, 32, 33] where:

$$E^f(d,q) = E(d,q) - E(pure) + \sum_l (\Delta n)_i \mu_i + q[E_v + \varepsilon_F] + E^q_{Cor}. \tag{1}$$

Here, the energy of the supercell with the defect is represented by $E(d,q)$, the energy of the supercell before the defect is introduced is represented by $E(pure)$ and $(\Delta n)_i$ represents the difference in the type l atoms between the defective supercells and pristine and the supercell. The energy of the valence band maximum (VBM) is represented by E_V and μ_i is the chemical potential of the added or removed l atom. The dielectric constant of silicon is obtained from ref [34], and this was used to calculate the electrostatic corrections presented by E^q_{Cor}. The Corrections For Formation Energy and EigenValues for charged defect simulations Package (CoFFEE) [35] was used in calculating the E^q_{Cor}. Afterwards the minimum energy needed in separating a defect pair in to a separate non-interacting defect which is known as the binding energy, is evaluated according to the approach of ref [36, 33].

$$E_b = \sum_i E^f_{isolated} - E^f_{defect-complex,} \tag{2}$$

where the summation of the energy of formation of the separate non-interacting defects is the $\sum_i E^f_{isolated}$ and the energy of the defect complexes is $E^f_{defect-complex}$. If we assume two different charge states given as q and q', respectively, the Fermi energy for which the energy of formation of the two charge states is the same, i.e., $\epsilon(q/q')$, is called the charge state transition energy level, and is given by [31, 33]:

$$\epsilon(q/q') = \frac{E^f(d,q;\varepsilon_F = 0) - E^f(d,q';\varepsilon_F = 0)}{q' - q.} \tag{3}$$

After the convergence test, the choice of cutt-off energy, the supercell size, and the k-point mesh was made. The test was carried out using the GGA functional with 50 Ry energy

cut-off to calculate the formation energy of the B_iO_{2i} defect complex at zero charge state. 64, 216, and 512-atom supercells were used with a k-point mesh of $3 \times 3 \times 3$, $2 \times 2 \times 2$ and $1 \times 1 \times 1$ respectively. The decrease in the energy of formation of the defect between the 512 and 216-atom supercell was less than 0.02 eV. We then proceed by using the 216-atom supercell,since the 512-atom supercell provided an accuracy that does not worth the additional computational expense. Using the 216-atom supercell and $2 \times 2 \times 2$ k-point mesh, the cut-off energy was varied from 10 Ry to 90 Ry with a step increase of 5 Ry. We find that the minimum energy of the relaxed structure only changes by less than 0.1 meV when cut-off energy increases beyond 45 Ry. Thus, by fixing the cut-off energy at this value and performing structural relaxation with k-point mesh of $2 \times 2 \times 2$ and $3 \times 3 \times 3$, we obtained the minimum energy difference of less than 0.002 eV for the two meshes. The silicon band gap was the calculated to be 1.18 eV using the HSE functional. The result was found to be close to the experimental value of 1.23 eV [37] and previous previous ab-initio studies [38, 39]. The defects were then constructed on the relaxed 216-atom pristine silicon cell. Using the 45 Ry energy cut-off and the $2 \times 2 \times 2$ grid of k-point mesh, the structure was refined until the total change in energy was less than 1×10^{-5} eV and forces were relaxed to below 0.001 eV/Å for all the calculations.

3. Structural relaxation and the binding energy

3.1. Structural Relaxation

The relaxed structures for the B_sO_i, B_iO_i, B_iC_s, B_sB_i $B_sO_iH_i$, $B_iO_iH_i$, $B_sC_iH_i$, and $B_sB_iH_i$ defect complexes are shown in Fig. 1. It should be noted that there are competing structures which are relatively unstable when hydrogen interstitial is introduced into the system. Therefore, the structures presented in the figure are the relatively more stable ones with H interstitial, at zero charge state. For each of the aforementioned defect, the bond-length between the impurity elements (i.e., B, O, and C) and the nearest-neighbour (NN) silicon atom before and after hydrogen passivation is presented in Table 1 and Table 2, respectively. When the defects are in neutral charge state (i.e., zero charge state), hydrogen

passivation has no significant effect on the bond-length between the impurity atoms and the NN silicon. However, for the ± 1 charge states of the defect, there is a significant relaxation such that there is a reduction in the bond lengths between the impurity atoms and the NN silicon atoms.This is generally the trend except in the cases of $B_iC_sH_i$ in $+1$ charge state where the $C - Si$ bond length increases, as well as in $B_sB_iH_i$ in -1 charge state where the the $B - Si$ bond length also increases.

3.2. Binding energy

The binding energy of the defects has been obtained using eqn. 3. and is presented in Table 3. The table also presents the reactions leading to the formation of the defect complexes. From the table, it can be seen that all the binding energies are positive, suggesting that the defect complexes are relatively more stable compared to their constituents. Our calculated binding energies are in qualitative agreement with experimental data since both indicate that the defect complexes are stable, as shown by the positive value of the binding energies. However, quantitatively, there is disagreement in the values of the binding energy. For example, for the non-passivated defects, the difference in the binding energy ranges from 0.05 eV to 0.3 eV. However, we note the following- the reported experimental value of binding energy is actually the binding free energy which includes the configurational entropy [21, 40]. The latter is not included in our calculation, and thus the quantitative difference between our calculated value of the experiment. Furthermore, for the passivated defect complexes, there are no experimental binding energy as yet, except for $B_iC_sH_i$ and $B_sB_iH_i$ as shown in the table. For these two H passivated complexes, the binding energy are in quantitative disagreement with the experimental data presumably due to the aforementioned reason. Furthermore, when our calculated DFT values of the binding energy is compared with previous DFT results, in particular for the B_iO_{2i} and B_sO_{2i} complexes, we note a difference of not more than 0.2 eV. This difference could be as a result of difference in supercell size, k-grid mesh and the energy cut-off used in the calculations. For example in Ref [40], supercell size of 64-atom was used in their calculations. In Ref [13] however, similar supercell size and k-point grid were used as ours, but their energy cut-off of 35 Ry

is smaller than the 45 Ry we have used in our calculations. Nevertheless, our results are in qualitative agreement in that the reported values of the binding energy suggest that the defect may be stable. Finally, for the B_iO_{2i} complex, our calculated value of binding energy of 0.76 eV and previous reported value of between 0.6 eV-1 eV suggest that the defect may indeed be stable as suggested by Voronkov *et al.* and Estreicher *et al.* [19, 40]. However, we would like to emphasize that this is not the only and sufficient reason to make conclusion about the stability of this particular defect.

3.3. Thermodynamic charge state transition levels

The thermodynamic charge state transition level is presented in Table 4. Also in Fig 2 and Fig 3, the plots of the formation energy of the defects as a function of the Fermi energy before and after hydrogen passivation are presented. For most of the defect complexes formed before hydrogen passivation, there is a good agreement between our predicted defect levels and the available experimental data, the difference being between 0.01-0.14 eV. After hydrogen passivation, our calculations predict a donor level that is in good agreement with the experimental data as well as previous theoretical results, for the B_sB_i defect complex in particular. For the rest of the defect complexes, after hydrogen passivation, our calculations show H has effect on the defect levels. Even though there is no experimental evidence for the hydrogen passivated defect complexes, our calculations show that hydrogen may passivate such defect complexes as studied in this work, since all the acceptor levels move towards the conduction band, and the donor levels move only slightly to the valence band. Finally, we would like to emphasize that although theory may predict double donor or double acceptor levels (i.e.,$+2/+1$ or $-1/-2$), these may not be identifiable via the DLTS experiment. It usually requires extra measurement such as field-dependent measurement, and even then, there is no certainty of seeing them. The reason being that shallow defect levels are usually absorbed by the valence or conduction band, and thus not seen by such a technique as the DLTS.

4. Summary

Density functional theory (DFT) calculations of defect complexes, including hydrogen-passivated defect complexes was carried out using the Heyd-Scuseria-Ernzehof functional (HSE) functional. We have shown that B_s, B_i, C_s, O_i and O_{2i} can combine to form a stable B_iO_i, B_iC_s, B_sO_i, B_sB_i, B_iO_{2i} and B_sO_{2i} defect complexes. After hydrogen passivation, stable $B_iO_iH_i$, $B_iC_sH_i$, $B_sO_iH_i$, $B_sB_iH_i$, $B_iO_{2i}H_i$ and $B_sO_{2i}H_i$ defect complexes can also be formed. Except for the B_sB_i defect complex, a shift of the donor levels towards the valence band for all the defect complexes was observed after hydrogen passivation. Similarly a shift in to the conduction band for all the acceptor levels were observed after hydrogen passivation. For the B_sB_i electrically inactive defect in particular, a (+1/0) donor level at E_V + 0.50 eV was observed, meaning that the defect electrically active. We conclude that hydrogen passivation has positive effect on the the electrical properties of these defect complexes.

5. Acknowledgement

This work is based on the research supported partly by National Research foundation (NRF) of South Africa (Grant specific unique reference number (UID) 98961). The opinions, findings and conclusion expressed are those of the authors and the NRF accepts no liability whatsoever in this regard. The authors acknowledge the Center For High Performance Computing (CHPC) Cape Town, South Africa for computational resources.

References

[1] H. Wang, A. Chroneos, C. Londos, E. Sgourou, U. Schwingenschlögl, Applied Physics Letters 103 (5) (2013) 052101.

[2] S.-R. Christopoulos, H. Wang, A. Chroneos, C. A. Londos, E. N. Sgourou, U. Schwingenschlögl, Journal of Materials Science: Materials in Electronics 26 (3) (2015) 1568–1571.

[3] N. Cowern, G. Mannino, P. Stolk, F. Roozeboom, H. Huizing, J. Van Berkum, F. Cristiano, A. Claverie, M. Jaraiz, Physical Review Letters 82 (22) (1999) 4460.

[4] L. Pelaz, M. Jaraiz, G. Gilmer, H.-J. Gossmann, C. Rafferty, D. Eaglesham, J. Poate, Applied physics letters 70 (17) (1997) 2285–2287.

[5] D. Eaglesham, T. Haynes, H.-J. Gossmann, D. Jacobson, P. Stolk, J. Poate, Applied physics letters 70 (24) (1997) 3281–3283.

[6] R. a. Scholz, U. Gösele, J.-Y. Huh, T. Tan, Applied physics letters 72 (2) (1998) 200–202.

[7] H. Osten, B. Heinemann, D. Knoll, G. Lippert, H. Rücker, Journal of Vacuum Science & Technology B: Microelectronics and Nanometer Structures Processing, Measurement, and Phenomena 16 (3) (1998) 1750–1753.

[8] H. Rücker, B. Heinemann, W. Röpke, R. Kurps, D. Krüger, G. Lippert, H. Osten, Suppressed diffusion of boron and carbon in carbon-rich silicon, Applied Physics Letters 73 (12) (1998) 1682–1684.

[9] J. Zhu, T. D. Dela Rubia, L. Yang, C. Mailhiot, G. H. Gilmer, Physical Review B 54 (7) (1996) 4741.

[10] W. Windl, M. Bunea, R. Stumpf, S. Dunham, M. Masquelier, Physical review letters 83 (21) (1999) 4345.

[11] J. Troxell, G. Watkins, Physical Review B 22 (2) (1980) 921.

[12] P. Mooney, L. Cheng, M. Süli, J. Gerson, J. Corbett, Physical Review B 15 (8) (1977) 3836.

[13] X. Chen, X. Yu*, X. Zhu, P. Chen, D. Yang, Applied physics Express 6 (1) (2013) 041301.

[14] J. Schmidt, K. Bothe, Physical review B 69 (2) (2004) 024107.

[15] K. Bothe, R. Sinton, J. Schmidt, Progress in Photovoltaics: Research and Applications 13 (4) (2005) 287–296.

[16] K. Bothe, J. Schmidt, Journal of Applied Physics 99 (1) (2006) 013701.

[17] J. Adey, R. Jones, D. Palmer, P. Briddon, S. Öberg, Physical review letters 93 (5) (2004) 055504.

[18] M.-H. Du, H. M. Branz, R. S. Crandall, S. Zhang, Physical review letters 97 (25) (2006) 256602.

[19] V. V. Voronkov, R. Falster, Journal of Applied Physics 107 (5) (2010) 053509.

[20] C. G. Van de Walle, J. Neugebauer, Annu. Rev. Mater. Res. 36 (2006) 179–198.

[21] J. Adey, R. Jones, P. Briddon, Applied physics letters 83 (4) (2003) 665–667.

[22] J. Heyd, G. E. Scuseria, M. Ernzerhof, The Journal of chemical physics 118 (18) (2003) 8207–8215.

[23] A. V. Krukau, O. A. Vydrov, A. F. Izmaylov, G. E. Scuseria, The Journal of chemical physics 125 (22) (2006) 224106.

[24] P. Deak, B. Aradi, T. Frauenheim, E. Janzen, A. Gali, Physical Review B 81 (15) (2010) 153203.

[25] J. Kusima, J. Ojanen, J. Enkovara, T. Rantala, Physical Review B 82 (11) (2010) 115106.

[26] P. Giannozzi, S. Baroni, N. Bonini, M. Calandra, R. Car, C. Cavazzoni, D. Ceresoli, G. L. Chiarotti, M. Cococcioni, I. Dabo, et al., Journal of physics: Condensed matter 21 (39) (2009) 395502.

[27] C. Hartwigsen, S. Gœdecker, J. Hutter, Physical Review B 58 (7) (1998) 3641.

[28] S. Goedecker, M. Teter, J. Hutter, Physical Review B 54 (3) (1996) 1703.

[29] H. Monkhorst, J. Pack, Special points for brillouin-zone integrations.

[30] S. Zhang, J. E. Northrup, Physical review letters 67 (17) (1991) 2339.

[31] C. Freysoldt, B. Grabowski, T. Hickel, J. Neugebauer, G. Kresse, A. Janotti, C. G. Van de Walle, Reviews of modern physics 86 (1) (2014) 253.

[32] Y. Kumagai, F. Oba, Physical Review B 89 (19) (2014) 195205.

[33] A. Abdurrazaq, W. Meyer, Physica B: Condensed Matter 572 (2019) 238–241.

[34] J. Paier, M. Marsman, G. Kresse, Physical Review B 78 (12) (2008) 121201.

[35] M. H. Naik, M. Jain, Computer Physics Communications 226 (2018) 114–126.

[36] G. Zollo, Y. Lee, R. Nieminen, Journal of Physics: Condensed Matter 16 (49) (2004) 8991.

[37] J. Robertson, Band offsets of wide-band-gap oxides and implications for future electronic devices 18 (3) (2000) 1785–1791.

[38] J. Heyd, J. E. Peralta, G. E. Scuseria, R. L. Martin, The Journal of chemical physics 123 (17) (2005) 174101.

[39] J. Paier, M. Marsman, K. Hummer, G. Kresse, I. C. Gerber, J. G. Ángyán, The Journal of chemical physics 124 (15) (2006) 154709.

[40] M. Sanati, S. Estreicher, Physical Review B 72 (16) (2005) 165206.

[41] J. Adey, R. Jones, D. W. Palmer, P. R. Briddon, S. Öberg, Physical Review B 93 (2004) 0555504.

[42] A. Carvalho, R. Jones, J. Coutinho, P. Briddon, Journal of Physics: Condensed Matter 17 (17) (2005) L155.

[43] J. Schmidt, K. Bothe, Physical review B 69 (2) (2004) 024107.

[44] S. Fatima, C. Jagadish, J. Lalita, S. B. G, H. j, Appl. Phys. 85 (1999) 2562.

Table 1: The relaxed bond length between the impurity atoms (B, O, C, H) and the nearest neighbour (NN) Si atoms for the defects having $-1, 0$, and 1 charge states. All distances are in Å.

Defect	Bonds	Bond length		
		-1	0	$+1$
B_iO_i	B−Si	2.265	2.156	2.804
	O−Si	1.805	1.792	2.605
B_iC_s	B−Si	2.202	2.093	2.741
	C−Si	2.060	2.232	2.220
B_sO_i	B−Si	2.047	2.036	2.284
	O−Si	1.840	1.827	2.640
B_sB_i	B−Si	2.038	2.027	2.275
	B−Si	2.180	2.071	2.719
B_i	B−Si	2.265	2.156	2.804
	B−Si	2.180	2.071	2.719
B_iO_{2i}	O−Si	1.731	1.718	2.431
	O−Si	1.724	1.711	2.524
	B−Si	2.047	2.036	2.293
B_sO_{2i}	O−Si	1.840	1.827	2.447
	O−Si	1.962	1.832	2.542

Table 2: The relaxed bond length between the impurity atoms (B, O, C, H) and the nearest neighbour (NN) Si atoms in hydrogen passivated defects having $-1, 0$, and 1 charge states. All distances are in Å.

Defect	Bonds	Bond length		
		-1	0	$+1$
$B_iO_iH_i$	B−Si	1.964	2.156	2.145
	O−Si	1.780	1.792	1.833
	H−Si	2.295	2.177	2.714
$B_iC_sH_i$	B−Si	1.901	2.093	2.025
	C−Si	2.350	2.232	2.769
	H−Si	2.339	2.179	2.614
	B−Si	1.884	2.036	2.024
$B_sO_iH_i$	O−Si	1.814	1.827	1.868
	H−Si	2.336	2.175	2.027
	B−Si	2.189	2.027	2.041
$B_sB_iH_i$	B−Si	1.705	2.071	1.759
	H−Si	2.337	2.178	2.029
B_iH_i	B−Si	1.964	2.156	2.145
	H−Si	2.332	2.177	2.028
	B−Si	1.879	2.071	2.060
$B_iO_{2i}H_i$	O−Si	1.705	1.718	1.759
	O−Si	1.698	1.711	1.752
	H−Si	2.375	2.215	2.066
	B−Si	1.874	2.036	2.050
$B_sO_{2i}H_i$	O−Si	1.814	1.827	1.868
	O−Si	1.819	1.832	1.873
	H−Si	2.363	2.203	2.054

Table 3: Binding energy E_b in eV for the defect complexes. The E_b is compared with the available experimental and previous theoretical data.

Defect	Study	Reaction	E_b
B_iO_i	This study	$B_i + O_i$	0.36
	Experiment [21]	$B_i + O_i$	0.60
$B_iO_iH_i$	This study	$B_iO_i + H_i$	0.19
B_iC_s	This study	$B_i + C_s$	0.90
	Experiment [21]	$B_i + C_s$	1.20
$B_iC_sH_i$	This study	$B_iC_s + H_i$	1.80
	Experiment [21]	$B_iC_s + H_i$	2.86
B_sO_i	This study	$B_s + O_i$	0.26
$B_sO_iH_i$	This study	$B_sO_i + H_i$	0.05
B_sB_i	This study	$B_s + B_i$	0.19
	Experiment [21]	$B_s + B_i$	Unspecified
$B_sB_iH_i$	This study	$B_sB_i + H_i$	0.92
	Experiment [21]	$B_sB_i + H_i$	1.60
B_i	This study	−	−
B_iH_i	This study	$B_i + H_i$	0.47
B_iO_{2i}	This study	$B_i + O_{2i}$	0.76
	Previous DFT [13, 40]	$B_i + O_{2i}$	0.96, 0.55, 0.61
$B_iO_{2i}H_i$	This study	$B_iO_{2i} + H_i$	0.89
B_sO_{2i}	This study	$B_s + O_{2i}$	0.43
	Experiment [41]	$B_s + O_{2i}$	0.38
	Previous DFT [40]	$B_s + O_{2i}$	0.54
$B_sO_{2i}H_i$	This study	$B_sO_{2i} + H_i$	0.59

Table 4: Charge state transition level for the defect complexes in eV.

Defect	Methods	(+2/+1)	(+1/0)	(0/−1)
B_iO_i	Experiment [12]	−	E_C −0.27	−
	Experiment [42]	−	E_C −0.23	−
	Marker Method [21]	−	E_C −0.22	−
	This study	−	E_C −0.26	−
$B_iO_iH_i$	This study	E_V + 0.14	E_V + 0.41	−
B_iC_s	Experiment [21, 42]	−	E_V + 0.29	−
	Maker Method [21]	−	E_V + 0.24	−
	This study	E_V + 0.20	E_V + 0.28	E_C − 0.08
$B_iC_sH_i$	This study	E_V + 0.11	E_V + 0.16	E_C − 0.03
B_sO_i	Experiment [43]	−	E_c − 0.49	−
	This study	E_V + 0.41	E_C − 0.54	E_C − 0.49
$B_sO_iH_i$	This study	E_V + 0.23	E_V + 0.33	−
B_sB_i	Experiment [21]	−	−	−
	This study	−	−	−
$B_sB_iH_i$	Experiment [44]	−	E_V + 0.51	−
	Marker method [21]	−	E_V + 0.56	−
	This study	−	E_V + 0.50	−
B_i	Experiment [11]	−	E_C −0.15	E_C −0.45
	This study	−	E_C −0.26	E_C −0.33
B_iH_i	This study	−	E_V + 0.37	E_C −0.07
B_iO_{2i}	Experiment [13]	−	E_C −0.41	−
	Maker Method [40]	−	E_C −0.48	−
	This study	−	E_C − 0.43	−
$B_iO_{2i}H_i$	This study	−	E_V + 0.51	−
B_sO_{2i}	Experiment [40]	−	E_C − 0.41	−
	Marker method [40]	−	E_C −0.50	−
	This study	E_V + 0.47	E_C − 0.39	E_C − 0.30
$B_sO_{2i}H_i$	This study	E_V + 0.30	E_V + 0.46	−

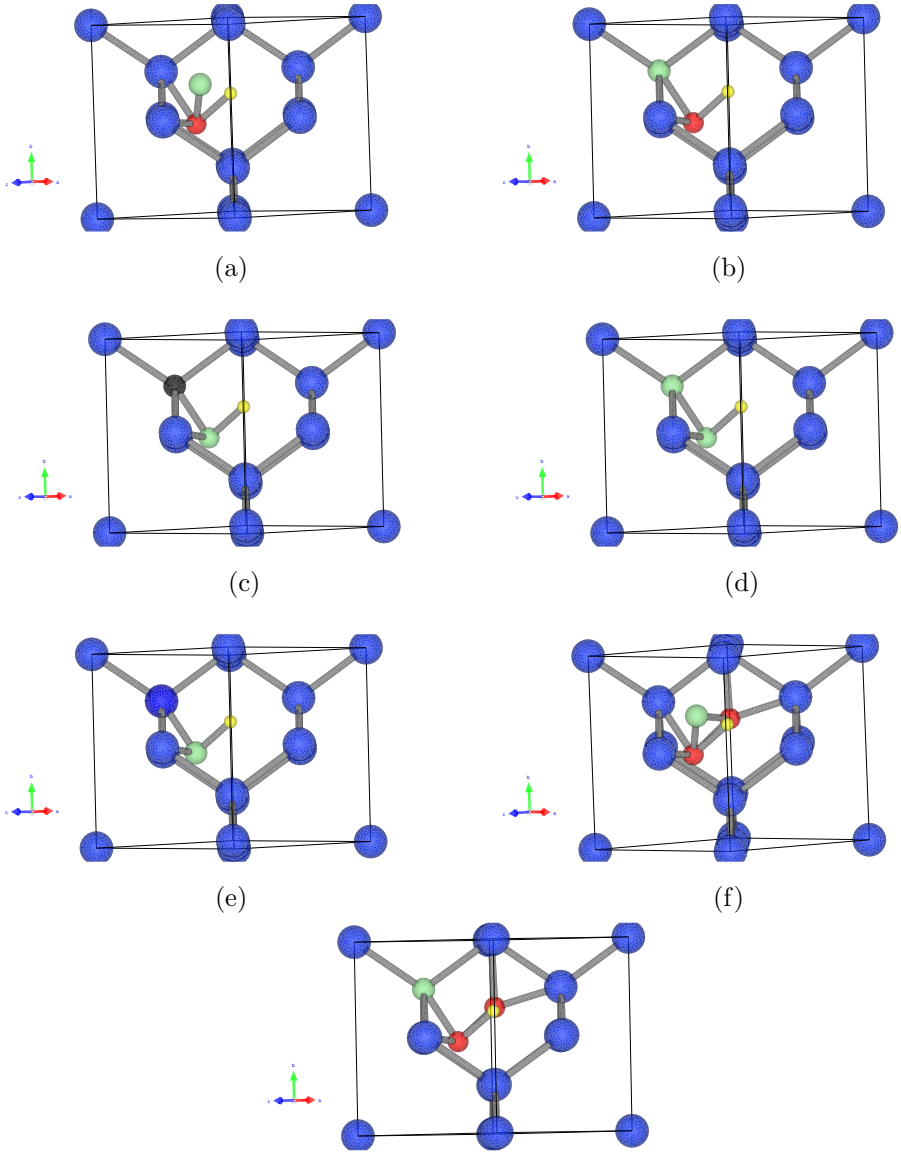

Figure 1: The relaxed geometric structure of the (a) $B_iO_iH_i$ (b) $B_sO_iH_i$ (c) $B_iC_sH_i$, (d) $B_sB_iH_i$ (e) B_iH_i (f) $B_iO_{2i}H_i$ and (g) $B_sO_{2i}H_i$ defect complexes. The blue balls represent silicon atoms, the black balls represent carbon, the red balls represent atoms oxygen, the yellow balls represent hydrogen atoms and the green ball represent boron atoms respectively.

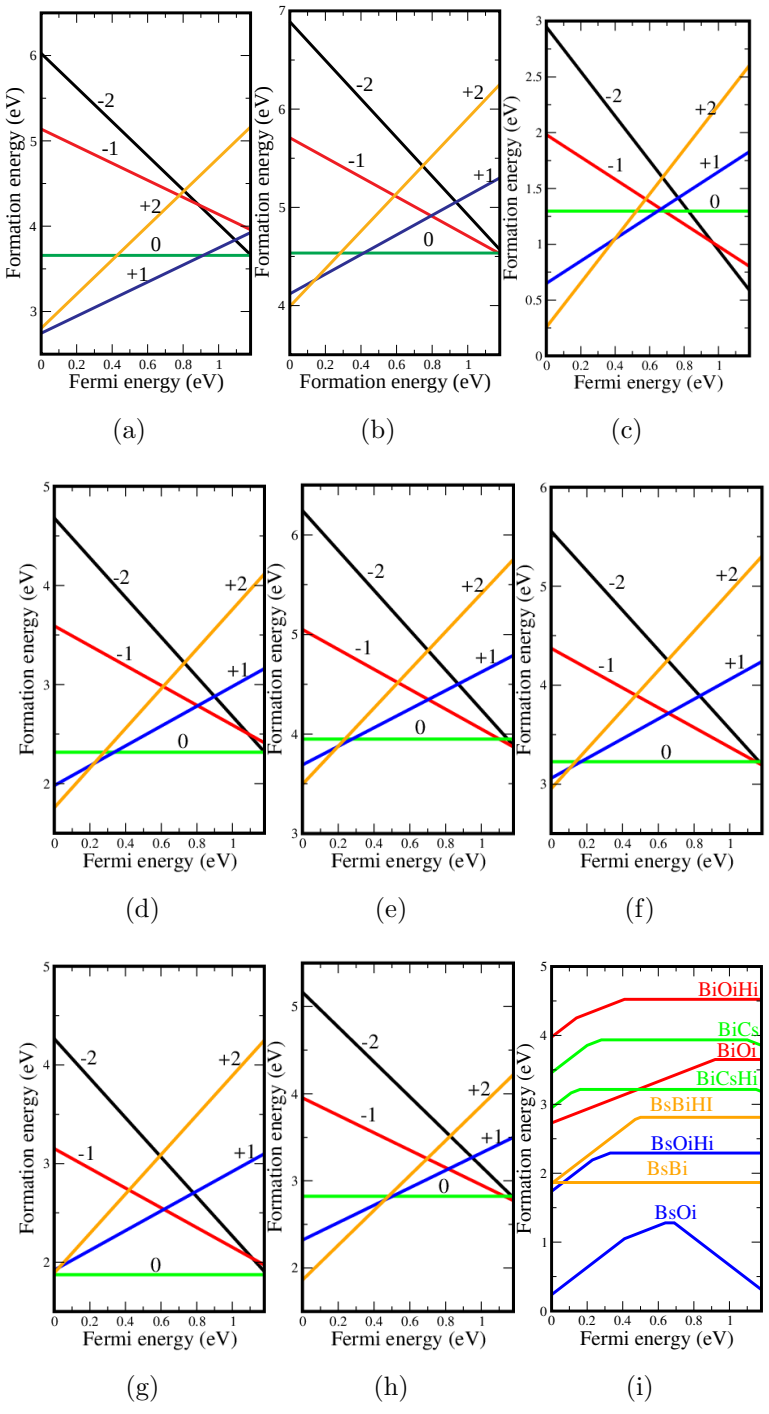

Figure 2: The formation energy as a function of the Fermi energy for the (a) B_iO_i (b) $B_iO_iH_i$, (c) B_sO_i (d) $B_sO_iH_i$ (e) B_iC_s (f) $B_iC_sH_i$ (g) B_sB_i (h) $B_sB_iH_i$ and (i) the thermodynamic stable region for all the defect complexes.

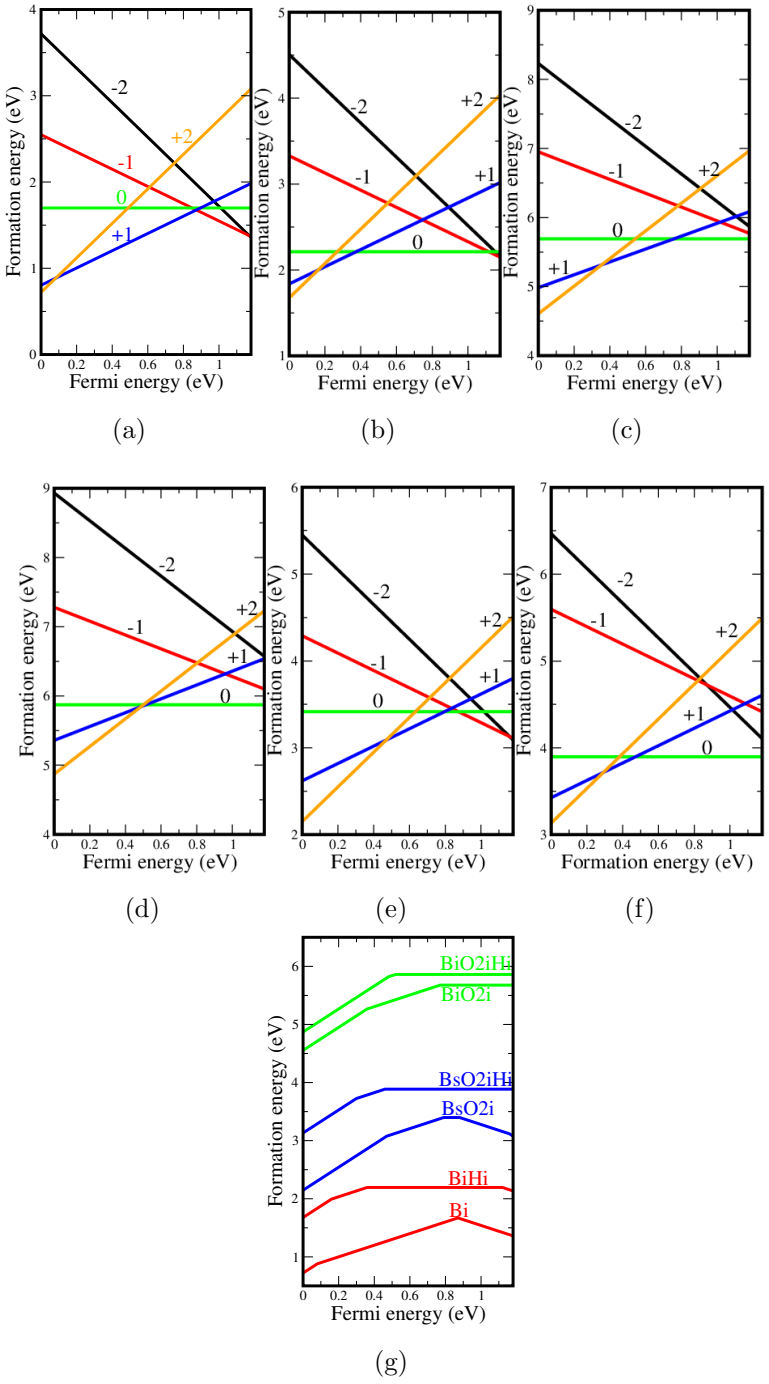

Figure 3: The for the formation energy as a function of the Fermi energy for the (a) B_i (b) B_iH_i, (c) B_iO_{2i} (d) $B_iO_{2i}H_i$ (e) B_sO_{2i} (f) $B_sO_{2i}H_i$ and (g) The thermodynamic stable regions for the defect complexes.